

Spectral method for bending analysis of rectangular functionally graded plates

Amina Hammou^{1,*}, Youssef Hilali^{1,2}, Said Mesmoudi³, Radouane Boujmal¹, Omar Askour⁴, and Oussama Bourihane¹

¹Laboratory of Mechanical Engineering, Faculty of Sciences and Technology Fez, Sidi Mohamed Ben Abdellah University, Fez, Morocco.

²Hassan First University of Settat, Faculty of Sciences and Techniques, 26000, Settat, Morocco.

³Hassan First University of Settat, National School of Applied Sciences, LISA Laboratory, Berrechid 26100, Morocco.

⁴Mathematics, Computer Science and Communication Systems Laboratory, National School of Applied Sciences of Safi, Cadi Ayyad University, Sidi Bouzid, BP 63, Safi-46000, Morocco.

Abstract. This study investigates the bending behavior of functionally graded rectangular plates using the spectral collocation method to offer precise modeling. We apply the First-order Shear Deformation Theory (FSDT) to accurately capture the effects of shear deformation in our plate behavior models. The effectiveness of the proposed method is demonstrated by a comparison of the results obtained with those of literature.

Keywords: Functionally graded materials, First order shear deformation Theory, Asymptotic numerical method, Bending analysis.

1 Introduction

Functionally Graded Material (FGM) is a composite material characterized by a controlled variation in composition and properties throughout its volume [1]. The thickness direction of FGM is systematically graded using a power-law distribution based on volume fractions of constituents.

Extensive research has been conducted on analyzing the behavior of functionally graded plates and shells Reddy [2], Cheng and Batra [3] and other researchers [1, 4–8].

In structural engineering, the FSDT for plates is a refined plate theory that extends the Classical Theory [9]. In contrast to the Classical Theory, which assumes plates to be thin and neglects the effects of transverse shear deformation, the FSDT takes into account the influence of shear deformation in a first-order approximation.

Meshless methods, including the spectral method that employs Chebyshev polynomials, simplify the modeling process, enhance accuracy, and accelerate convergence, presenting a viable alternative to traditional approaches. [7, 8, 10–12]. The spectral collocation method expands the solution to a differential equation using a global interpolant, distinguishing it from local interpolant-based methods like finite element or finite difference.

*e-mail: amina.hammou@usmba.ac.ma

The Asymptotic Numerical Method (ANM) solves complex nonlinear problems by developing solutions in the form of asymptotic series. Unlike local iterative methods like Newton-Raphson, ANM makes it possible to analyze nonlinear behavior over large parameter domains, which is particularly useful for the study of bifurcations. This method effectively solves nonlinear problems with hyperelastic materials, reducing tangent matrix decompositions and requiring no special treatment for instabilities or limit points [13]. The proposed approach, which combines the spectral collocation method with the numerical asymptotic method, offers several advantages, including high accuracy and effective management of complex boundary conditions, thus providing flexibility for modeling various scenarios in the analysis of functionally graded material (FGM) plates. Additionally, this approach reduces computational costs compared to traditional methods. However, it also has limitations, such as difficulties in handling non-smooth solutions, complexity in implementation, and potential risks of numerical instability in certain cases. These considerations underscore the need for careful evaluation of the application conditions for this approach. The Asymptotic Numerical Method offers high accuracy for nonlinear problems by combining analytical and numerical techniques, making it efficient in terms of computational resources by leveraging asymptotic behavior. However, its effectiveness depends on the presence of a small parameter, which may limit its applicability to certain problems, and the complexity of the method increases as higher-order corrections are considered.

The focus in this study is on investigating the linear bending behavior of rectangular plates with regular boundaries using the spectral meshless method. A thorough understanding of plate bending is essential for ensuring the stability and performance of various structural engineering applications. Driven by these factors, our objective is to develop a pseudospectral method based on Chebyshev polynomials for bending analyses of FGM plates. We will employ the FSDT theory that takes into account the influence of shear deformation in a first-order approximation that are neglected in the Classical theory in order to capture the elastic and anisotropic behavior of the plates.

Motivated by these factors, we aim to develop a Chebyshev polynomial-based spectral collocation method for the nonlinear bending analysis of Functionally Graded Material (FGM) plates. We will employ the First-order Shear Deformation Theory (FSDT) to capture the elastic and anisotropic behavior of the plates.

The paper is structured as follows: first, Section 2 provides a concise overview of the functionally graded materials, integrates the FSDT through the strong formulation, and exposes the equilibrium equations. Moving on to Section 3, we introduce the spectral method based on Chebyshev polynomials and the asymptotic numerical method (MAN) in the 4th section. Following this, Section 5 is dedicated to presenting the numerical results obtained from the examples utilized. Finally, in Section 6, we present the key concluding remarks.

2 Theoretical formulation

2.1 Functionally graded material properties

Consider a thin rectangular plate made of FG Material with in-plane dimensions L and l , and thickness h . The plate has a rectangular cross-section with a Cartesian coordinate system (O, x, y, z) established in the middle plane, where the origin O is positioned at one corner, as illustrated in Fig. 1. The material on the top surface at $z = h/2$ is ceramic-rich, gradually transitioning to a metal-rich composition at the bottom surface of the plate at $z = -h/2$.

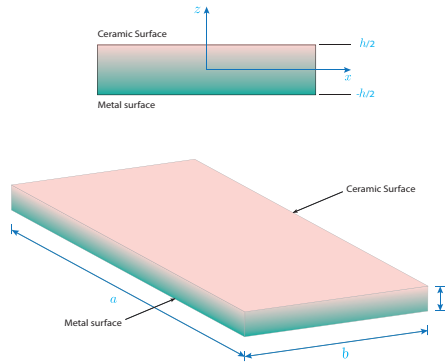


Figure 1: FGM plate [1].

An assumption is made about the ceramic volume fraction V_c with respect to the coordinate z . This assumption is expressed as :

$$V_c(z) = \left(\frac{1}{2} + \frac{z}{h}\right)^k \tag{1}$$

Here, h is the thickness of the structure, and $k \geq 0$ is the power law index defining the metal variation through the plate thickness.

The effective material characteristics, encompassing the isotropic FGM's Poisson ratio ν , mass density ρ , and elasticity modulus E , are described by combining the material constants of ceramic and metallic components through the following expression :

$$P(z) = V_m P_m + V_c P_c \tag{2}$$

The volume fractions V_c and V_m satisfy the relationship $V_c + V_m = 1$

2.2 Fundamental Equations

In FSDT, the displacements u_M , v_M , and w_M at a point $M(x, y, z)$ within the plate are expressed as functions of the mid-plane displacements u , v , w , and the first-order partial derivatives of the transverse deflection with respect to the spatial coordinates x and y . The relationships are given by the following equations:

$$\begin{cases} u_M = u + z\beta_x, \\ v_M = v + z\beta_y, \\ w_M = w. \end{cases} \tag{3}$$

Here, u , v , and w represent the mid-plane displacements, while β_x and β_y are the first-order partial derivatives of the transverse deflection w with respect to the spatial coordinates x and y , respectively.

The entire problem-solving system can be summarized as follows:

$$\left\{ \begin{array}{l} N = C_0 \left([D^m][H]g^u + \frac{1}{2}[D^m][A(g^w)]g^w \right) + C_1[D^m][H]g^\beta \\ M = C_1 \left([D^m][H]g^u + \frac{1}{2}[D^m][A(g^w)]g^w \right) + C_2[D^m][H]g^\beta \\ Q = C_0 D^s g^w + C_0 D^s \beta \\ \operatorname{div} N = 0 \\ \operatorname{div} Q + [N, w] = -\lambda f_3 \\ \operatorname{div} M - Q = 0 \\ nN = \lambda T^d \\ nQ + \langle B(w) \rangle N = -\lambda Q^d \\ nM = -\lambda M^d \end{array} \right. \quad (4)$$

with,

$${}^T \mathbf{g} = \langle g^u \quad g^\beta \quad g^w \rangle \quad (5)$$

where M, N and Q are the generalized stresses, \mathbf{g} is the gradient vector, f is the external force vector, D_m and D_s are a symmetrical dimensionless behavior matrix and strain coefficient respectively, u is the displacement vector and g is the gradient vector. The coefficients C_i are equal to :

$$C_i = \int_z z_i E(z) dz, \quad i = 0, 1, 2 \quad (6)$$

3 Asymptotic numerical method

To apply the procedure approach, we apply the following steps:

We use a Taylor series expansion to express the unknowns as functions of a dimensionless scalar parameter a :

$$\mathbf{u} = u_j + \sum_{k=0}^N a^k \mathbf{u}_k, \quad \lambda = \lambda_j + \sum_{k=0}^N a^k \lambda_k$$

The unknowns are connected to the parameter a by the following relationship :

$$\langle \mathbf{u} - \mathbf{u}_0, \mathbf{u}_1 \rangle + \lambda_1(\lambda - \lambda_0) = a$$

The expansions are substituting into the nonlinear equations to create a sequence of linear systems based on powers of a . So, using Asymptotic Numerical Method (ANM) for solving the non-linear resulting equations, we find:

Order $k = 1$:

$$\left\{ \begin{array}{l} N_1 = C_0 \left([D^m][H]g_1^u + [D^m][A(g_0^w)]g_1^w \right) + C_1[D^m][H]g_1^\beta \\ M_1 = C_1 \left([D^m][H]g_1^u + [D^m][A(g_0^w)]g_1^w \right) + C_2[D^m][H]g_1^\beta \\ Q_1 = C_0 D^s g_1^w + h D^s \beta_1 \\ \operatorname{div} N_1 = 0 \\ \langle \operatorname{div} \rangle Q_1 + [N_0, w_1] + [N_1, w_0] = -\lambda_1 f_3 \\ \operatorname{div} M_1 - Q_1 = 0 \\ nN_1 = \lambda_1 T^d \\ \operatorname{div} Q_1 + \langle B(w_0) \rangle N_1 + \langle B(w_1) \rangle N_0 = -\lambda_1 Q^d \\ nM_1 = -\lambda_1 M^d \end{array} \right. \quad (7)$$

Order $k \geq 2$:

$$\left\{ \begin{array}{l} N_k = C_0 \left([D^m][H]g_k^u + [D^m][A(g_0^w)]g_k^w \right) + C_1 [D^m][H]g_k^\beta + C_0 [D^m] \sum_{r=1}^{k-1} [A(g_r^w)]g_{k-r}^w \\ M_k = C_1 \left([D^m][H]g_k^u + [D^m][A(g_0^w)]g_k^w \right) + C_2 [D^m][H]g_k^\beta + C_1 [D^m] \sum_{r=1}^{k-1} [A(g_r^w)]g_{k-r}^w \\ Q_k = C_0 D^s g_k^w + h D^s \beta_k \\ \text{div} N_k = 0 \\ \langle \text{div} \rangle Q_k + [N_0, w_k] + [N_k, w_0] = -\lambda_k f_3 - \sum_{r=1}^{k-1} [N_k, w_{(k-r)}] - [N_k^m, w_0] \\ \text{div} M_k - Q_k = 0 \\ n N_k = \lambda_k T^d \\ \text{div} Q_k + \langle B(w_0) \rangle N_k + \langle B(w_k) \rangle N_0 = -\lambda_k Q^d - \sum_{r=1}^{k-1} \langle B(w_k) \rangle N_{(k-r)} - \langle B(w_0) \rangle N_k^m \\ n M_k = -\lambda_k M^d \end{array} \right. \quad (8)$$

The unknowns are then discretized using Chebyshev polynomials to solve the system precisely as presented in section 4. Then, we calculate the upper limit a_{\max} for the parameter a :

$$a_{\max} = \left(\frac{\epsilon_d \|\mathbf{u}_1\|}{\|\mathbf{u}_j\|} \right)^{\frac{1}{j-1}}$$

The solutions are defigning at a_{\max} as the new starting point for the next computation. The validity range for this point determined after recalculating the expansions. The process is repeated by using the current results to set new starting points for subsequent computations, recalculating expansions for each branch. Iterating is continued until the desired solution range is achieved or the system indicates no further valid solutions are possible.

4 Spectral collocation Method

This section introduces the spectral method for constructing shape functions to solve differential equations. The interpolant is given by:

$$u(\mathbf{x}_j) \approx P_{N-1}(\mathbf{x}) = \sum_{j=1}^N \frac{\alpha(\mathbf{x})}{\alpha(\mathbf{x}_j)} \phi_j(\mathbf{x}) u_j \quad (9)$$

Here, $\{\mathbf{x}\}$ represents distinct interpolation nodes, $\alpha(\mathbf{x})$ is a weight function, and $f_j = f(\mathbf{x}_j)$. The interpolating functions $\phi(\mathbf{x})$ satisfy $\phi_j(\mathbf{x}) = \delta_{jk}$, and $p_{N-1}(\mathbf{x})$ is an interpolant of the function $u(\mathbf{x})$.

Numerical differentiation is expressed as:

$$u^{(l)} = D^{(l)} u \quad (10)$$

The Chebyshev interpolating function, constrained to Chebyshev nodes and constant weights, is defined as:

$$P_{N-1}(\mathbf{x}) = \sum_{j=1}^N \phi_j(\mathbf{x}) u_j \quad (11)$$

Where:

$$\phi_j(\mathbf{x}) = \frac{(-1)^j}{c_j} \frac{(1-x^2) T'_{N-1}(\mathbf{x})}{(N-1)^2 (x-x_j)} \quad (12)$$

Here, $T_{N-1}(\mathbf{x})$ is the Chebyshev polynomial of degree $N - 1$, with $c_1 = c_N = 2$ and $c_2 = \dots = c_{N-1} = 1$. D is the Chebyshev differentiation matrix, where $D^{(l)} = (D^{(1)})^l$.

For 2D grids, the storage layout and computation of partial derivatives are discussed. The field values are stored in a 1D array of size $N_{2D} = n_1 n_2$, with differentiation matrices

$D_1^{(l)} = D_{n1 \times n1}^{(l)}$ and $D_2^{(l)} = D_{n2 \times n2}^{(l)}$. Using the Kronecker product, the 2D differentiation matrices are constructed as:

$$\begin{aligned} \bar{D}^{(l)1} &= D_1^{(l)} \otimes I_2, \\ \bar{D}^{(l)2} &= I_1 \otimes D_2^{(l)} \end{aligned} \tag{13}$$

Here, I_α is the identity matrix of size $n_\alpha \times n_\alpha$, and $D^{(l)}$ is the 2D differentiation matrix of size $N_{2D} \times N_{2D}$. The spectral derivative computation for a 2D field is given by the matrix multiplication:

$$\partial_\alpha v = \bar{D}_\alpha^{(l)} .v. \tag{14}$$

The use of 2D differentiation matrices facilitates the derivation of the tangent operator, to discretize the system presented in Eq.(4).

In the present study the following sets of boundary conditions are used:

Simply supported (SSSS):

$$\begin{aligned} u_0 = w_0 = \beta_y = 0 & \quad \text{at} \quad x = 0 \text{ and } x = L \\ v_0 = w_0 = \beta_x = 0 & \quad \text{at} \quad y = 0 \text{ and } y = l \end{aligned} \tag{15}$$

Clamped (CCCC):

$$u_0 = v_0 = w_0 = \beta_x = \beta_y = 0 \quad \text{at} \quad x = 0, x = L, y = 0 \text{ and } y = l \tag{16}$$

5 Numerical results and discussion

In this study, two test examples of simply supported and clamped FG plates were examined to ensure the accuracy and effectiveness of the proposed method. The proposed algorithm was validated and compared to results available in the literature.

5.1 Example 1 : simply supported FG plate

In this example, the analysis concerns a square plate of side $L = l = 0.2m$ and thickness $h = 0.1m$, with different volume fraction indices. The plate is assumed to be simply supported on all its edges. The results are presented in terms of non-dimensional parameters, namely: central deflection (w/h), load parameter $q = \frac{q_0 L^4}{E_m h^4}$, and thickness coordinate $\bar{z} = \frac{z}{h}$. Here, q denotes the intensity of the applied mechanical load. The FGM plate is made of a mixture of aluminum (metal) and zirconia (ceramic): $E_m = 70GPa$ and $E_c = 151GPa$. The Poisson's ratio $\nu = 0.3$ for simplicity. The dimensionless central deflection as a function of load parameters and arrangement of figures are presented according to those of Reddy to allow direct comparison. Good agreement between the two sets of results is observed, as illustrated in Figure 5. The accuracy of the proposed formulation is compared to the results obtained by Reddy [2], who uses third-order shear deformation plate theory with von Karman-type geometric nonlinearity.

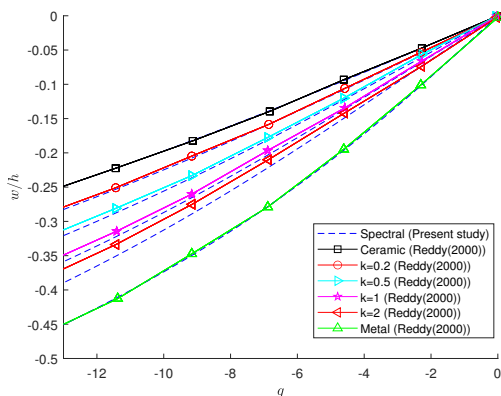


Figure 2: Comparison of load–deflection curve for SSSS zirconia/aluminum square FGM plate subjected to uniform pressure.

5.2 Example 2 : clamped FG plate

In this example, we analyze the nonlinear bending of a square FGM plate composed of silicon nitride and stainless steel (SUS304), as studied by Yang and Shen [14]. The upper surface of the plate is enriched with ceramic, while the lower surface is enriched with metal. The material properties are as follows: $E_m = 207.78GPa$ for SUS304 and $E_c = 322.27GPa$ for Si. Poisson’s ratio ν is assumed to be constant and equal to 0.28. The non-dimensional parameters used are: the central deflection w/h , the load parameter $q = \frac{q_0 L^4}{E_m h^4}$, and the coordinate thickness ($\bar{z} = \frac{z}{h}$). The plate is completely clamped on all its edges with a width-thickness ratio ($b/h = 10$), for $k = 0$ (ceramic), $k = 2$, and $k = \infty$ (metal). The non-dimensional deflection as a function of the load parameter is chosen similar to that used by Yang and Shen [14].

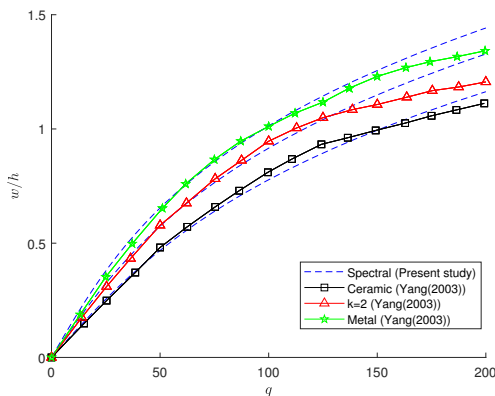


Figure 3: Comparison of load–deflection curve for CCCC silicon nitride/stainless steel square FGM plate subjected to uniform pressure.

Figures 2 and 3 illustrate the variations of \bar{w} at the center of the plate with respect to the normalized parameter load (q) in the presence of uniform loading for several power-law index k varying from ceramic ($k = 0$) to metal ($k = \infty$).

6 Concluding remarks

The nonlinear bending of functionally graded plates is analyzed by applying the FSDT theory. For spatial discretization, the Chebyshev spectral collocation method is employed. Dimensionless deflections are evaluated under uniform loading conditions for two types of boundary conditions of ceramic-metal plates. The results highlight the effectiveness of the spectral method based on Chebyshev polynomials in the study of nonlinear bending of rectangular plates. In future work, we plan to extend the spectral collocation method to analyze the buckling behavior of functionally graded plates and other geometries, such as circular ones.

References

- [1] A. Hammou, Y. Hilali, S. Mesmoudi, R. Boujmal, O. Bourihane, *Mathematics and Computers in Simulation* **218**, 112 (2024)
- [2] J. Reddy, *International Journal for numerical methods in engineering* **47**, 663 (2000)
- [3] Z. Cheng, R. Batra, *Archives of Mechanics* **52**, 143 (2000)
- [4] K. Zahari, Y. Hilali, S. Mesmoudi, O. Bourihane et al., *Review and comparison of thin and thick FGM plate theories using a unified buckling formulation*, in *Structures* (Elsevier, 2022), Vol. 46, pp. 1545–1560
- [5] K. Zahari, Y. Hilali, S. Mesmoudi, O. Bourihane et al., *Materials Today Communications* **38**, 108094 (2024)
- [6] A. Hammou, Y. Hilali, S. Mesmoudi, R. Boujmal, O. Bourihane, *Hermite-type PIM approach for buckling analysis of L-shaped FGM thin plates*, in *2023 3rd International Conference on Innovative Research in Applied Science, Engineering and Technology (IRASET)* (IEEE, 2023), pp. 1–5
- [7] S. Mesmoudi, M. Rammane, Y. Hilali, O. Askour, O. Bourihane, *Variable RPIM and HOCM coupling for non-linear buckling and post-buckling analysis of transverse FG sandwich beams*, in *Structures* (Elsevier, 2023), Vol. 53, pp. 895–907
- [8] S. Mesmoudi, Y. Hilali, M. Rammane, O. Askour, O. Bourihane, *Thin-Walled Structures* **185**, 110614 (2023)
- [9] J.N. Reddy, *Mechanics of laminated composite plates and shells: theory and analysis* (CRC press, 2003)
- [10] Y. Hilali, O. Bourihane, *A mixed MLS and Hermite-type MLS method for buckling and postbuckling analysis of thin plates*, in *Structures* (Elsevier, 2021), Vol. 33, pp. 2349–2360
- [11] Y. Hilali, O. Bourihane, *Engineering with Computers* **38**, 3171 (2022)
- [12] S. Mesmoudi, O. Askour, M. Rammane, O. Bourihane, A. Tri, B. Braikat, *International Journal for Numerical Methods in Engineering* **123**, 6111 (2022)
- [13] S. Nezamabadi, H. Zahrouni, J. Yvonnet, *Computational mechanics* **47**, 77 (2011)
- [14] J. Yang, H.S. Shen, *Composites Part B: Engineering* **34**, 103 (2003)